Smart Structures and Systems, *Vol. 21, No. 4 (2018) 435-448*
DOI: https://doi.org/10.12989/sss.2018.21.4.435

Bayesian ballast damage detection utilizing a modified evolutionary algorithm

Qin Hu[1,2a], Heung Fai Lam[*3], Hong Ping Zhu[1,2b] and Stephen Adeyemi Alabi[3c]

[1]*School of Civil Engineering and Mechanics, Huazhong University of Science and Technology, Wuhan, Hubei, PR China, 430074*
[2]*Hubei Key Laboratory of Control Structure, Huazhong University of Science and Technology, Wuhan, Hubei, PR China, 430074*
[3]*Department of Architecture and Civil Engineering, City University of Hong Kong, HKSAR, China*

(Received June 3, 2017, Revised February 28, 2018, Accepted March 1, 2018)

Abstract. This paper reports the development of a theoretically rigorous method for permanent way engineers to assess the condition of railway ballast under a concrete sleeper with the potential to be extended to a smart system for long-term health monitoring of railway ballast. Owing to the uncertainties induced by the problems of modeling error and measurement noise, the Bayesian approach was followed in the development. After the selection of the most plausible model class for describing the damage status of the rail-sleeper-ballast system, Bayesian model updating is adopted to calculate the posterior PDF of the ballast stiffness at various regions under the sleeper. An obvious drop in ballast stiffness at a region under the sleeper is an evidence of ballast damage. In model updating, the model that can minimize the discrepancy between the measured and model-predicted modal parameters can be considered as the most probable model for calculating the posterior PDF under the Bayesian framework. To address the problems of non-uniqueness and local minima in the model updating process, a two-stage hybrid optimization method was developed. The modified evolutionary algorithm was developed in the first stage to identify the important regions in the parameter space and resulting in a set of initial trials for deterministic optimization to locate all most probable models in the second stage. The proposed methodology was numerically and experimentally verified. Using the identified model, a series of comprehensive numerical case studies was carried out to investigate the effects of data quantity and quality on the results of ballast damage detection. Difficulties to be overcome before the proposed method can be extended to a long-term ballast monitoring system are discussed in the conclusion.

Keywords: Bayesian model updating; Bayesian model class selection; modified evolutionary algorithm; railway ballast; damage detection

1. Introduction

Regular inspection and maintenance of railway tracks is a major task for permanent way engineers. A possible cause of track deterioration is ballast fouling, which results in the poor drainage of tracks and reduces the overall strength and stiffness of the ballast layer in supporting the sleepers (Selig and Waters 1994). Highly fouled ballast will not only significantly affect its drainage ability, but will also lead to track settlement. In this study, ballast damage (or ballast deterioration) is defined as the stiffness reduction of ballast in supporting the sleeper. The detection of ballast damage is a challenging task in railway maintenance.

In the last decade, smart structure health monitoring has obtained researchers' attention (Fujino *et al.* 2009, Jo *et al.* 2012, Nagayama *et al.* 2007, Yuen and Lam 2006), especially, the automatic structural damage detection using vibration data has become one of the major research areas in civil engineering due to the advancement in technologies of sensors (Ni *et al.* 2011, 2012, Meyer *et al.* 2010). Comprehensive reviews in vibration-based damage detection for civil engineering structures are available in references (Salawu 1997, Fan and Qiao 2011). However, the extension of this idea to the detection of damage for railway ballast is new and challenging.

Lam and colleagues proposed to use the vibration data from the sleeper to detect the damage of the underlying ballast (Lam *et al.* 2010). Due to the reduction in ballast stiffness, it is possible to detect the deterioration of ballast by utilizing model updating technique via measured vibration of the sleeper (Lam *et al.* 2012). It must be pointed out that there are uncertainties associated with the measured quantities and so as the identified model parameters due to the problems of measurement noise and modelling error. The level of uncertainties depends on the amount of information that can be extracted from the available measurement and the complexity of the model class employed in the model updating process (this directly related to the number of uncertain model parameters to be identified). It must be pointed out that there is no theoretically rigorous deterministic method to deal with this uncertainty problem, and the probabilistic approach provides a feasible solution in handling it.

Bayesian inference can update the uncertainties of the model parameters (Jeffreys 1961, Box and Tiao 1973) and

*Corresponding author, Associate professor
E-mail: paullam@cityu.edu.hk
[a] Ph.D.
E-mail: husthuqin@hust.edu.cn
[b] Professor
E-mail: hpzhu@hust.edu.cn
[c] Ph.D. candidate,
E-mail: stephen.alabi@my.cityu.edu.hk

ISSN: 1738-1584 (Print), 1738-1991 (Online)

provide a feasible identification solution for the purpose of structural health monitoring and crack growth prediction (Yuen 2010, An *et al.* 2011, Kuok and Yuen 2012). The original formulation of the Bayesian statistical system identification framework is in the time domain (Beck and Katafygiotis 1998), and it was extended to modal domain by Vanik and colleagues (Vanik *et al.* 2000). In 2014, Lam and colleagues developed the Bayesian ballast damage detection method which utilized the measured natural frequencies and mode shapes of the rail-sleeper-ballast system. The new method was verified through experimental case studies in a full-scale in-door test panel (Lam *et al.*, 2014). However, it is well known that the minimization problem involved in the model updating process is extremely complicated. There may be many local minima in the parameter space of interest. Some of them may lead to models with the same outputs at the measured degrees-of-freedom (non-uniqueness problem). As a result, an effective numerical method is in demand for identifying the important regions in the parameter space (i.e., the regions correspond to high probability). For developing a practical ballast damage detection method, it is very important to study the effects of the quantity (e.g., the number of measured modes to be considered in the model updating process) and quality (e.g., the level of measurement noise) of measured data on the results of ballast damage detection. This is one of the main purposes of this paper to study this effect through a series of comprehensive case studies.

The long-term goal of this research is to develop a smart system for continuous monitoring of the "health" condition of railway ballast through measuring the train-induced vibration of a selected number of in-situ sleepers along the targeted ballasted track. This paper focuses on the ballast damage detection of a single in-situ sleeper, which is one of the key components of this smart system.

The originalities of this paper are (1) to develop the modified evolutionary algorithm (and so as the hybrid optimization method) in addressing the optimization problem in model updating process; (2) to numerically and experimentally verify the proposed ballast damage detection method; and (3) to study the effects of the data quantity and quality on the results of ballast damage detection.

2. Background theories and proposed methodology

The class of rail-sleeper-ballast model for the purpose of ballast damage detection is first presented. The core part of the methodology is the Bayesian approach, which can be divided into Bayesian model class selection and Bayesian model updating. It follows by the development of the two-stage hybrid optimization method with the modified evolutionary algorithm. The posterior PDF of ballast stiffness at different regions can then be calculated by the proposed ballast damage detection method. Details of each component of the proposed methodology are presented in the following sub-sections.

2.1 Modelling of the rail-sleeper-ballast system

The three main components of an in-situ sleeper are the two rails, the sleeper and the underlying ballast. The rails carry the vertical load from the train and distribute it to the sleepers. The sleepers are embedded into the ballast and the load is transferred through the ballast to the foundation. The ballast is tightly tamped around the sleepers to keep the track precisely levelled and aligned. Appropriate modelling of the ballasted track is the key component of a model-based ballast damage detection method.

From the literature, the two rails can be modelled as two springs (Kaewunruen and Remennikov 2009, Berggren, 2009) or two masses (Lam *et al.* 2012) in the rail-sleeper-ballast system. Recently, Lam and colleagues (Hu and Lam 2012, Lam *et al.* 2014, Hu *et al.* 2015) experimentally verified that it is feasible to model the two rails as two individual masses. In this study, their values are calculated by $m_L=\theta_L\times m_r$ and $m_R=\theta_R\times m_r$, where m_r is the nominal value of rail mass and θ_L and θ_R are the scaling factors (to be considered as uncertain parameters in the model updating process) for the left and right mass, respectively. The sleeper on ballast are modelled as a Timoshenko beam on an elastic foundation based on the finite element method. The railway ballast is considered by the discrete modeling method (Lam *et al.* 2014) in this study, namely, the ballast is divided into several discrete regions (e.g., N_d regions for the given model class) and the ballast stiffness in each region is assumed to be a constant. For each region, a dimensionless scaling factor θ_i, for $i = 1, 2, \ldots, N_d$, is used to scale the nominal ballast stiffness k_b. These N_d scaling factors are considered as uncertain model parameters (i.e., minimization variables) in model updating. Due to the aging effect, the Young's modulus of the sleeper may also vary, and another scaling factor θ_E is used to scale its nominal value. As a result, there are N_d+3 uncertain model parameters, which are grouped into an uncertain model parameter vector $\boldsymbol{\theta} = [\theta_1, \theta_2, \ldots \theta_{Nd}, \theta_E, \theta_L, \theta_R]$ in the model updating process.

The formulation of a Timoshenko beam on an elastic foundation in reference (Krenk 2001) was adopted in the proposed method. Furthermore, the consistent mass matrix (Przemieniecki 1985) was employed in the dynamic analysis. The element stiffness and mass matrices are used to assemble the system stiffness and mass matrices. The modal parameters, such as, natural frequencies and mode shapes of the system, can be calculated by solving the eigenvalue problem of the system stiffness and mass matrices (Lam *et al*. 2012, 2014).

2.1 Bayesian model class selection and model updating for ballast damage detection

The core of the proposed methodology is the Bayesian approach. In this sub-section, emphasis will be put on how the existing theories of Bayesian model class selection and Bayesian model updating be integrated to the proposed methodology for ballast damage detection.

2.2.1 Bayesian model class selection for ballast damage detection

To be self-contain, the Bayesian model class selection

method is briefly reviewed here. Interested readers are redirected to references (Beck and Yuen 2004, Lam *et al.* 2007, 2008, Lam and Yin 2010) for the complete formulations.

The Bayesian model class selection method is used to select the most plausible model class among $N_{\max}$ given model classes. This is done by calculating the probability of each model class conditional on the set of measurement $\boldsymbol{D}$ and the subjective judgement of the user u, $p(\boldsymbol{M}_j \mid \boldsymbol{D}, u)$ for j = 1 to $N_{\max}$. The model class with the highest probability is the most plausible model class. In the proposed ballast damage detection method, j is considered as the number of regions under the sleeper. For example, $\boldsymbol{M}_1$ represents the model class of rail-sleeper-ballast system with only one ballast region (undamaged). $\boldsymbol{M}_2$ and $\boldsymbol{M}_3$ represent the model classes with two and three, respectively, equal ballast regions. The probability of a model class conditional on the set of measurement can be expressed as

$$P\left(\boldsymbol{M}_j \left| \boldsymbol{D}, u\right.\right) = \frac{p\left(\boldsymbol{D}\left|\boldsymbol{M}_j, u\right.\right) P\left(\boldsymbol{M}_j \left| u\right.\right)}{p\left(\boldsymbol{D}\left|u\right.\right)}, \quad \text{for } j = 1, \ldots, N_{\max} \qquad (1)$$

where $P(\boldsymbol{M}_j| u)$ is the prior probability on the model classes M_j for j = 1, 2, …, N_{max}. In general, it is assumed to be a constant equal to $1/N_{\max}$. $p(\boldsymbol{D}| \boldsymbol{M}_j, u)$ is the evidence, which is proportional to the total probability of the model class if a constant prior probability is assumed. The subjective judgement u is dropped out in later formulations to simplify the formulation. In locally identifiable cases (Beck and Katafygiotis, 1998), the posterior PDF for $\boldsymbol{\theta}_j$ for a given set of measured data $\boldsymbol{D}$ can be approximated accurately by a Gaussian distribution, then the evidence $p(\boldsymbol{D}| \boldsymbol{M}_j)$ can be asymptotically approximated by using Laplace's method (Papadimitriou *et al.* 1997)

$$p\left(\boldsymbol{D}\left|\boldsymbol{M}_j\right.\right) \approx p\left(\boldsymbol{D}\left|\hat{\boldsymbol{\theta}}_j, \boldsymbol{M}_j\right.\right)(2\pi)^{\frac{N_j}{2}}\, p\left(\hat{\boldsymbol{\theta}}_j \left| \boldsymbol{M}_j\right.\right)\left|\boldsymbol{H}_j\left(\hat{\boldsymbol{\theta}}_j\right)\right|^{-\frac{1}{2}}, \quad \text{for } j = 1, \ldots, N_{\max} \qquad (2)$$

where $\hat{\boldsymbol{\theta}}_j$ represents the most probable model in the model class $\boldsymbol{M}_j$, the compositions of $\hat{\boldsymbol{\theta}}_j$ for ballast damage detection are $\hat{\theta}_1$, $\hat{\theta}_2$, …, $\hat{\theta}_j$, $\hat{\theta}_E$, $\hat{\theta}_L$, $\hat{\theta}_R$. N_j is the number of uncertain parameters in $\hat{\boldsymbol{\theta}}_j$, and is equal to j + 3 in this study. $\boldsymbol{H}_j\left(\hat{\boldsymbol{\theta}}_j\right)$ is the Hessian matrix. The evidence in Eq. (2) consists of two factors, the likelihood factor, $p\left(\boldsymbol{D}\left|\hat{\boldsymbol{\theta}}_j, \boldsymbol{M}_j\right.\right)$, and the Ockham factor, $(2\pi)^{\frac{N_j}{2}}\, p\left(\hat{\boldsymbol{\theta}}_j \left| \boldsymbol{M}_j\right.\right)\left|\boldsymbol{H}_j(\hat{\boldsymbol{\theta}}_j)\right|^{-\frac{1}{2}}$. The balance between the likelihood and Ockham factors allow the selection of the most plausible model class (Beck and Yuen 2004, Muto and Beck 2008, Cao and Wang 2014, Worden and Hensman 2012).

To use the Bayesian model class selection formulation in ballast damage detection, a computationally efficient sequential algorithm was developed for identifying the most plausible model class $\boldsymbol{M}_j$ without defining $N_{\max}$ (Lam *et al.* 2014). Owing to the space limitation, the sequential algorithm, which consists of a series of iteration steps, is briefly reviewed here. Fig. 1 shows the schematic of the algorithm. The algorithm begins by testing the simplest class of model with $j = 1$, which stands for the one-region model class. In a general iteration step, the algorithm compares the evidence of the model class $\boldsymbol{M}_j$ with that of model class $\boldsymbol{M}_{j+1}$. If the evidence of the model class $\boldsymbol{M}_j$ is larger than that of the model class $\boldsymbol{M}_{j+1}$, then the algorithm stops and the model class $\boldsymbol{M}_j$ is selected. Otherwise, the algorithm will assign $j = j + 1$ and repeat the calculation of the evidence and comparison. Interested readers are redirect to reference (Lam *et al.* 2014) for details of the sequential algorithm.

2.2.2 Integrating Bayesian model updating for ballast damage detection

Bayesian model updating aims in calculating the posterior PDF of the uncertain model parameters $\boldsymbol{\theta}_j$ conditional on a given set of measured data, $\boldsymbol{D}$, and a given class of models, $\boldsymbol{M}_j$, which is selected by Bayesian model class selection. To simplify the expressions, the subscript j will be discarded in the following formulation, and the set of uncertain parameters and the selected model class are denoted as $\boldsymbol{\theta}$ and $\boldsymbol{M}$, respectively. By following the Bayes' theorem, the posterior PDF of uncertain model parameters can be expressed as (Vanik *et al.* 2000, Lam *et al.* 2014)

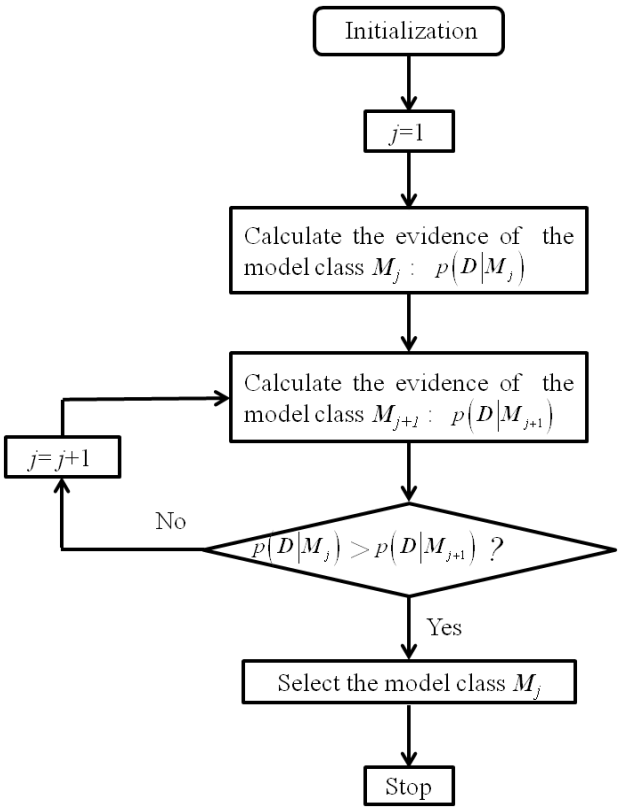

Fig. 1 The sequential algorithm for identifying the most probable model class for ballast damage detection (Hu 2015)

$$p\left(\boldsymbol{\theta}\middle|\boldsymbol{D},\boldsymbol{M}\right)=c\exp\left[-\frac{1}{2}J(\boldsymbol{\theta})\right] \tag{3}$$

Where c is a normalizing constant, and $J(\boldsymbol{\theta})$ is a positive definite measure-of-fit function shows the discrepancy between the measured and model-predicted modal parameters. In this paper, it is given by

$$J(\boldsymbol{\theta})=\sum_{r=1}^{N_m}\sum_{n=1}^{N_s}\sum_{k=1}^{N_k}\left[\frac{\left(\hat{\omega}_{r,n,k}^2-\omega_r^2(\boldsymbol{\theta})\right)^2}{\delta_{\hat{\omega}_r}{}^2}+\frac{\boldsymbol{\varphi}_r^T(\boldsymbol{\theta})\boldsymbol{\Gamma}^T\left(\mathbf{I}-\hat{\boldsymbol{\psi}}_{r,n,k}\hat{\boldsymbol{\psi}}_{r,n,k}^T\right)\boldsymbol{\Gamma}\boldsymbol{\varphi}_r(\boldsymbol{\theta})}{\delta_{\hat{\boldsymbol{\psi}}_r}{}^2\left\|\boldsymbol{\Gamma}\boldsymbol{\varphi}_r(\boldsymbol{\theta})\right\|^2}\right] \tag{4}$$

where N_m, N_s and N_k are the number of modes, data sets, and impact locations to be considered in the model updating process; $\hat{\omega}_{r,n,k}$ is the measured squared natural frequencies, $\omega_r(\boldsymbol{\theta})$ is the calculated squared natural frequency of the r-th mode from a given model $\boldsymbol{\theta}$; $\hat{\boldsymbol{\psi}}_{r,n,k}$ is the measured mode shape, $\boldsymbol{\varphi}_r(\boldsymbol{\theta})$ is the r-th mode calculated mode shape. The selection matrix $\boldsymbol{\Gamma}$ consists of only 1 and 0 that picks the observed DOFs from the model-predicted mode shapes to match the measured ones, $\|\bullet\|$ is the Euclidean norm. $\delta_{\hat{\omega}_r}{}^2$ and $\delta_{\hat{\boldsymbol{\psi}}_r}{}^2$ are the posterior variance of the squared natural frequencies and mode shapes following the Bayesian framework. The first and second terms of the J function in Eq. (4) correspond to the discrepancy in natural frequencies and mode shapes, respectively, of different modes and different measurement sets. Under the identifiable model updating problem, the posterior PDF in Eq. (3) can be approximated by a weighted sum of multivariance Gaussian distributions which are centered at the optimal solutions of the J function in Eq. (4). Therefore, a computational efficient algorithm for locating all output-equivalent optimal solutions of the J function is essential for the success of Bayesian model updating, and so as the ballast damage detection in the proposed methodology.

2.3 Two-stage hybrid optimization method

For the minimization problem in model updating, there may have multiple minima in the parameter space of interest (non-uniqueness problem). Furthermore, there may exist many local minima. It is well-known that most deterministic optimization algorithms may be easily trapped by local minima, and they are not suitable to be directly adopted for model updating. Most probabilistic optimization algorithms are not focusing on identifying one minimum but on generating points "near" the minima. Therefore, they are not easily trapped by local minima. However, it usually takes large computational power and long computational time for the "near" minima points to converge to the global minima. In this paper, a two-stage hybrid optimization method was developed to overcome this difficulty. The proposed hybrid optimization method consists of two stages. The evolutionary strategy (Back 1996) was modified and used in the first stage to identify all important regions in the parameter space of interest (i.e., regions with high PDF values) in a relatively short time. In the second stage, deterministic numerical optimization algorithm is employed to accurately identify the "optimal" model in each important region (near each local minimum). These "optimal" models will be treated as the most probable models in the Bayesian model updating method for calculating the posterior PDF of uncertain parameters.

The formulation of the modified evolutionary algorithm is presented in the following. To start with, $\boldsymbol{\Theta}^{(g)}$ is defined to store all individuals in a general g-th generation

$$\boldsymbol{\Theta}^{(g)}=\left\{\boldsymbol{\theta}_1^{(g)}\quad\boldsymbol{\theta}_2^{(g)}\quad\cdots\quad\boldsymbol{\theta}_i^{(g)}\quad\cdots\quad\boldsymbol{\theta}_{N_p}^{(g)}\right\}^T \tag{5}$$

where N_p is the population size and g is the index for generation; $\boldsymbol{\theta}_i^{(g)}$ is the i-th individual in the g-th generation, which is defined as

$$\boldsymbol{\theta}_i^{(g)}=\left\{\theta_{1,i}^{(g)}\quad\theta_{2,i}^{(g)}\quad\cdots\quad\theta_{j,i}^{(g)}\quad\cdots\quad\theta_{N,i}^{(g)}\right\} \tag{6}$$

where N is the total number of uncertain model parameters. In the proposed method, $N = N_d + 3$, where N_d is the number of discrete ballast regions under the sleeper as defined in section 2.1.

One of the key components of the modified evolutionary algorithm is the way to generate children from the parents. In each generation, a child is generated by following a multivariable Gaussian distribution with the parent as the mean and a covariance matrix given by

$$\mathbf{C}^{(g)}=\begin{bmatrix}\delta_1^{(g)} & \alpha_{1,2}^{(g)} & \cdots & \alpha_{1,j}^{(g)} & \cdots & \alpha_{1,N}^{(g)}\\ \alpha_{2,1}^{(g)} & \delta_2^{(g)} & \cdots & \alpha_{2,j}^{(g)} & \cdots & \alpha_{2,N}^{(g)}\\ \vdots & \vdots & \ddots & \vdots & \ddots & \vdots\\ \alpha_{i,1}^{(g)} & \alpha_{i,2}^{(g)} & \cdots & \delta_i^{(g)} & \cdots & \alpha_{i,N}^{(g)}\\ \vdots & \vdots & \ddots & \vdots & \ddots & \vdots\\ \alpha_{N,1}^{(g)} & \alpha_{N,2}^{(g)} & \cdots & \alpha_{N,j}^{(g)} & \cdots & \delta_N^{(g)}\end{bmatrix} \tag{7}$$

where the elements $\delta_i^{(g)},\quad \text{for } i=1,\ldots,N$ and $\alpha_{i,j}^{(g)},\quad \text{for } i=1,\ldots,N;\ j=1,\ldots,N$ are given by

$$\boldsymbol{\delta}^{(g)}=\left\{\delta_1^{(g)}\quad\delta_2^{(g)}\quad\ldots\quad\delta_N^{(g)}\right\}^T \tag{8}$$

$$\boldsymbol{\alpha}^{(g)}=\begin{bmatrix}\alpha_{1,1}^{(g)} & \alpha_{1,2}^{(g)} & \cdots & \alpha_{1,j}^{(g)} & \cdots & \alpha_{1,N}^{(g)}\\ \alpha_{2,1}^{(g)} & \alpha_{2,2}^{(g)} & \cdots & \alpha_{2,j}^{(g)} & \cdots & \alpha_{2,N}^{(g)}\\ \vdots & \vdots & \ddots & \vdots & \ddots & \vdots\\ \alpha_{i,1}^{(g)} & \alpha_{i,2}^{(g)} & \cdots & \alpha_{i,i}^{(g)} & \cdots & \alpha_{i,N}^{(g)}\\ \vdots & \vdots & \ddots & \vdots & \ddots & \vdots\\ \alpha_{N,1}^{(g)} & \alpha_{N,2}^{(g)} & \cdots & \alpha_{N,j}^{(g)} & \cdots & \alpha_{N,N}^{(g)}\end{bmatrix} \tag{9}$$

The diagonal terms of $\boldsymbol{\alpha}^{(g)}$ are not used in the

calculation of the covariance matrix. The values of $\boldsymbol{\delta}^{(g)}$ and $\boldsymbol{\alpha}^{(g)}$ can be calculated based on their values in the previous generation (Back 1996)

$$\boldsymbol{\delta}^{(g)} = \boldsymbol{\delta}^{(g-1)} \exp\left(\tau_1 \mathbf{G}_{N,1} + \tau_2 \mathbf{G}_{1,1} \mathbf{I}_{N,1}\right) \tag{10}$$

$$\boldsymbol{\alpha}^{(g)} = \boldsymbol{\alpha}^{(g-1)} + \beta \mathbf{G}_{N,N} \tag{11}$$

where $\mathbf{G}_{N_1,N_2}$ is a random matrix of dimension N_1 by N_2 following a normal distribution with zero mean and unit variance; τ_1, τ_2, and β are algorithmic parameters, their values will be discussed later; and $\mathbf{I}_{N,1} = \{1, 1, \ldots, 1\}^T$ is a vector of unity with dimension N by 1. The children in the g-th generation can be generated by

$$d_i^{(g)}(j) = \boldsymbol{\theta}_i^{(g-1)} + \mathbf{N}(0, \mathbf{C}^g), \quad \text{for } i = 1,\ldots,N_p;\ j = 1,\ldots,N_c \tag{12}$$

where $\mathbf{N}(\mathbf{a},\mathbf{b})$ is a multivariable normal distribution with mean defined by $\mathbf{a}$ and covariance defined by $\mathbf{b}$. In the modified evolutionary algorithm, the j-th children for all the parents are stored in the variable

$$\mathbf{D}^{(g)}(j) = \left\{ d_1^{(g)}(j) \quad d_2^{(g)}(j) \quad \ldots \quad d_{N_P}^{(g)}(j) \right\}^T \tag{13}$$

In the g-th generation, all parents and children are grouped together and stored in the variable

$$\mathbf{P}^{(g)} = \left\{ \boldsymbol{\Theta}^{(g-1)} \quad \mathbf{D}^{(g)}(1) \quad \mathbf{D}^{(g)}(2) \quad \ldots \quad \mathbf{D}^{(g)}(N_c) \right\}^T \tag{14}$$

In $\mathbf{P}^{(g)}$, the best (with the smallest J values) N_p individuals are used to form $\boldsymbol{\Theta}^{(g)}$, which are the N_p individuals in the g-th generation.

To initialize, all algorithmic parameters must be defined as (Back 1996)

$$\tau_1 = \frac{1}{\sqrt{2\sqrt{N}}}, \quad \tau_2 = \frac{1}{\sqrt{2N}}$$

where N is the total number of uncertain parameters. In Eq. (11), $\beta = 0.0873$ (Back 1996) is used. In the first generation (g = 1), the covariance matrix in Eq. (7) with g = 1 is formed by

$$\begin{aligned} \boldsymbol{\delta}^{(1)} &= \delta_0 \mathbf{I}_{N,1} \\ \boldsymbol{\alpha}^{(1)} &= \alpha_0 \mathbf{I}_{N,N} \end{aligned} \tag{15}$$

where $\delta_0 = 3$ and $\alpha_0 = 0$ (Back, 1996) are used in this study, and $\mathbf{I}_{N,N}$ is an unity matrix (all $N \times N$ elements are unity). The stopping criterion is mathematically expressed as

$$\left| J_{\max} - J_{\min} \right| \le \varepsilon \tag{16}$$

where $J_{\min} = \min_{\boldsymbol{\theta} \in \boldsymbol{\Theta}^{(g)}} J(\boldsymbol{\theta})$, $J_{\max} = \max_{\boldsymbol{\theta} \in \boldsymbol{\Theta}^{(g)}} J(\boldsymbol{\theta})$, and $\varepsilon = 10^{-6}$ is used in this study.

Upon the completion of the modified evolutionary algorithm in the first stage, a set of individuals (points in the parameter space) can be obtained. When there are more than one local minimum with very similar objective function values, the samples will be concentrated in more than one important region (one important region for each local minimum). Since the J values for all points are available in all generations, the point with the smallest J value in each region can be identified. They will be considered as the initial trials in the series of deterministic numerical optimizations in the second stage.

2.4 The proposed procedure of ballast damage detection

After reviewing all background technologies, the procedure of the proposed ballast damage detection methodology is summarized as follows:

1. The time-domain vibration data of the possibly damaged in-situ sleeper is measured through roving hammer tests (with one accelerometer and one impact hammer with load cell). The accelerometer is fixed at the pre-defined measured DOF of the in-situ sleeper, and the impulses are applied through the impact hammer at the 11 pre-defined excitation DOFs (distributed along the center line of the in-situ sleeper) one by one (Lam *et al.* 2014).
2. The MODE-ID method (Beck 1978) is used to identify the modal parameters from the measured acceleration responses of the in-situ sleeper. The set of measurements ***D*** can be used for model class selection and model updating by the Bayesian approach. Other modal identification methods, such as the fast Bayesian FFT modal identification method (Au 2011, Zhang *et al.* 2015, Ni *et al.* 2015), can also be used.
3. By the Bayesian model class selection method and the sequential algorithm, the most plausible class of models can be identified conditional on the set of measurements ***D***.
4. By maximizing the posterior PDF of the uncertain model parameters conditional on the 'most plausible' model class and the set of measurements, the 'most probable' model can be identified by the two-stage hybrid optimization method. The posterior PDF of ballast stiffness can then be calculated.
5. By plotting the identified ballast stiffness distribution along the target in-situ sleeper, the ballast damage location and the corresponding damage extent can be observed (detected) graphically.

3. Numerical verification

A typical rail-sleeper-ballast system (see section 2.1) is employed in this section as the basic finite element model (FEM) for generating vibration data of the undamaged and various damaged cases. The nominal values of Young's modulus and density of the concrete sleeper are 38×10^9 N/m^2 and 2200 kg/m^3, respectively. The effects of the two rails are represented by two different concentrated masses on the beam. The nominal value of the rail mass and the ballast stiffness are set to be 42 kg and 315×10^7 N/m^2, respectively (Hu 2015).

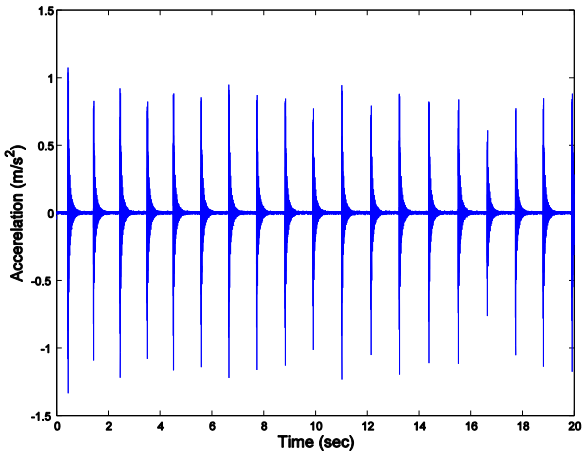

(a) Time-domain responses at pre-defined measured DOF

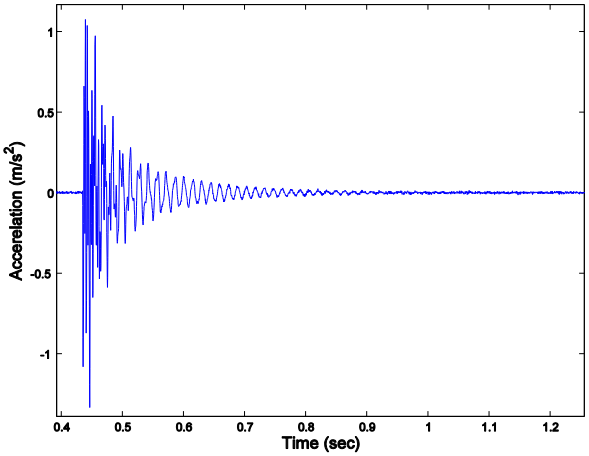

(b) Close up of the first impulse

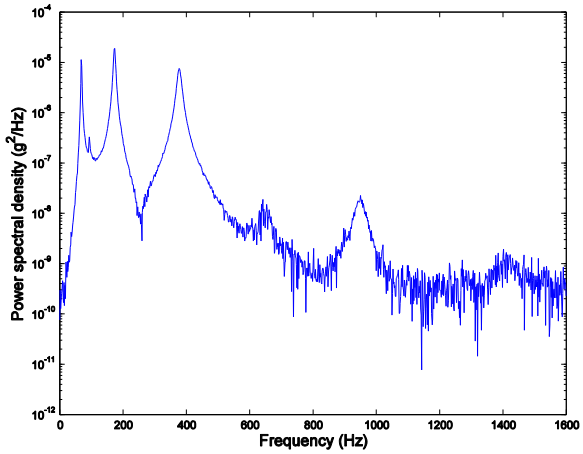

(c) Frequency domain response of the first impulse

Fig. 2 Sample of measured time and frequency domain response of the undamaged case

3.1 Numerical verification in undamaged case

To make the computer simulation representative, the parameters of the undamaged model of this numerical case studies was obtained from the model updating of the model class with uniform stiffness distribution under the sleeper utilizing impact hammer test results from a full-scale indoor test panel. The undamaged model is given by $\boldsymbol{\theta}_1 = [\theta_1, \theta_E, \theta_L, \theta_R] = [1.00, 1.05, 1.60, 1.56]$ (Hu 2015), where the subscript 1 shows that there is only one region under the sleeper implying that this is model class $\boldsymbol{M}_1$. Various damaged cases in the numerical case studies were simulated based on this undamaged model.

Impulsive forces were applied to the pre-defined excitation degree of freedoms (DOFs) of this model one-by-one and the time-domain responses at the sensor DOF were calculated by FEM with the assumption that the system is classically damped with a damping ratio of 2% (Hu 2015).

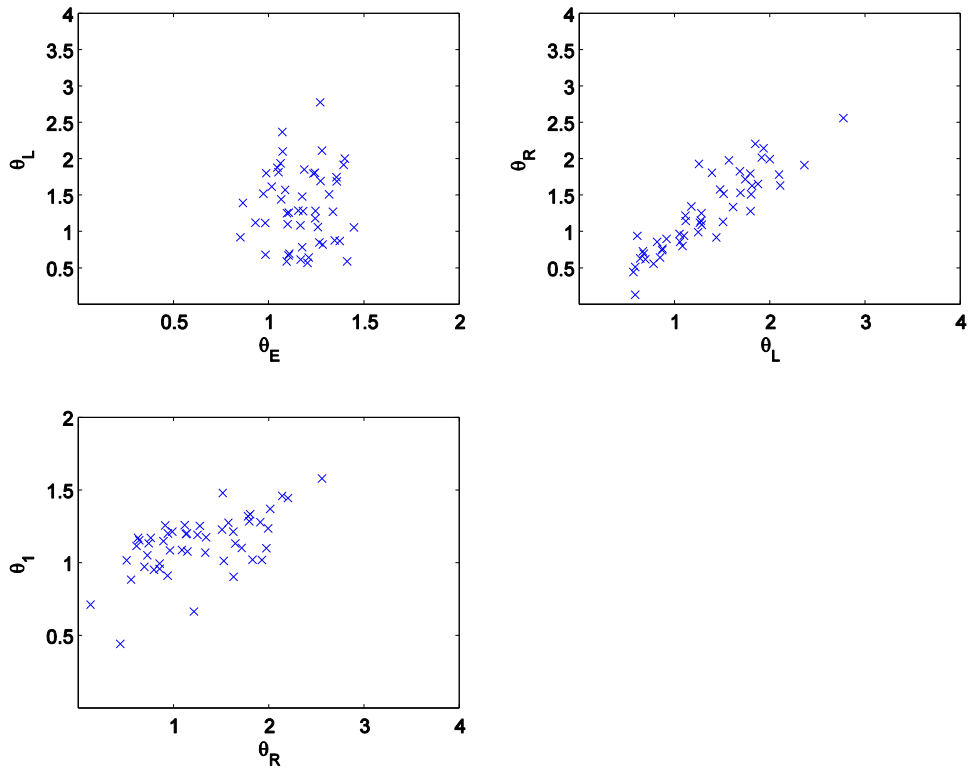

Fig. 3 The population of points generated by the modified evolutionary algorithm after 100 generations

To consider the effects of measurement noise, 1% of root mean square white noise was added to the calculated time-domain responses. It must be pointed out that a comprehensive case study on the effect of measurement noise level on the results of ballast damage detection is reported later in section 3.5.

The simulated time-domain response at the pre-defined measured DOF is shown in Fig. 2(a). The vibration test consists of many impulses (at the same input DOF). The duration between two impulses is long enough for the response of the system to delay to zero. To show more clearly about the measured acceleration response, Fig. 2(b) shows the close up of the first impulse in Fig. 2(a). The simulated time-domain responses with impact force at other DOFs look very similar, and they are not shown here. Fast Fourier Transform (FFT) was employed to transform the time-domain response to the frequency domain (see Fig. 2(c)). The peaks in Fig. 2(c) show the frequencies near the natural frequencies of the system, and they were employed as the initial trials for modal identification by MODE-ID. The natural frequencies and mode shapes of the first four modes were identified and used as the measured data for ballast damage detection.

The Bayesian model updating of the undamaged rail-sleeper-ballast system is employed as an example to illustrate the procedures of the proposed hybrid optimization method. In the first stage, 50 individuals were generated in the final generation as shown in Fig. 3. It is clear from the figure that there is only one important region in the parameter space of interest. Consider the distribution of samples along θ_E (i.e., Young's modulus of the sleeper).

The θ_E value of samples is very close to unity, and the result is relatively certain (the range of scattering points is relatively small). When compared to θ_E, the values for θ_L and θ_R (i.e., the left and right rail masses) are relatively uncertain. This is reflected by the relatively large range of scattering points. Finally, the value of θ_1 (i.e., the ballast stiffness) is also close to unity but the uncertainty should be lower than that of θ_L and θ_R but higher than that of θ_E. The point with the lowest J function value was used as the initial trial in the second stage of the hybrid method. Finally, the optimal model of the undamaged case was identified by Bayesian model updating, and the most probable model is given in Table 1. As expected, the identified model is very similar to the model employed for generating the measured data. The effect of introducing 1% of measurement noise is only very minor.

To generate different damaged cases, the ballast under the sleeper was divided into three regions with equal widths. They are denoted as Regions 1, 2 and 3 on the left, middle and right hand-sides of the sleeper, respectively. Ballast damage is simulated by a 50% reduction in ballast stiffness at the corresponding region. This is equal to multiply a factor of 0.5 to the ballast stiffness at the damaged region. In this numerical case study, two damaged cases were considered. The reductions in ballast stiffness of these two damaged cases were summarized in Table 2. Damaged case 1 considers the small damaged region case and the damage is simulated at Region 1, and damaged case 2 considers the large damaged region case and the damage is at Regions 1 and 2.

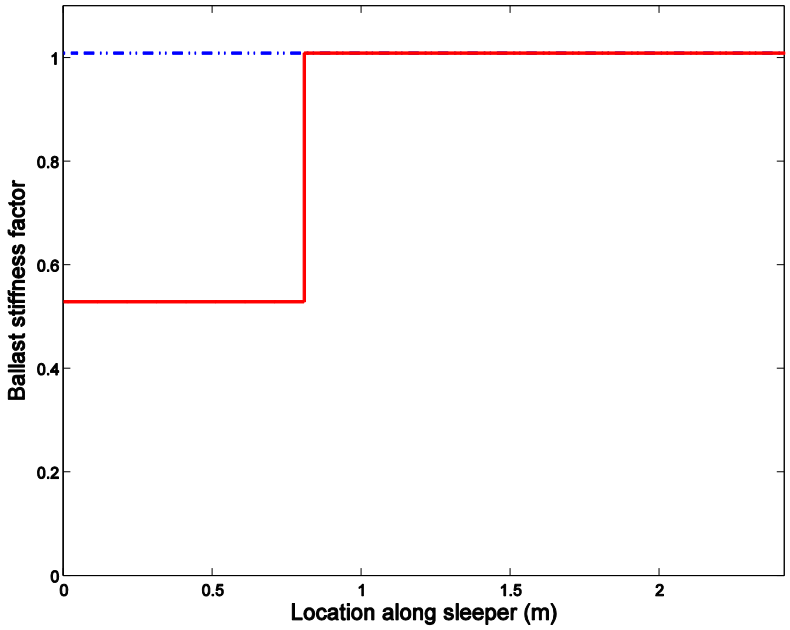

Fig. 4 Damage detection result in numerical damaged case 1

Table 1 Identified model parameters in undamaged case

Case	θ_1	θ_E	θ_L	θ_R
Undamaged	1.01	1.04	1.59	1.55

Table 2 Reductions in ballast stiffness in numerical damaged cases

Damaged case	Region 1	Region 2	Region 3
1	50%	---	---
2	50%	50%	---

3.2 Numerical verification in damaged case 1

The proposed Bayesian ballast damage detection method was conducted utilizing all four modes. As discussed previously, Bayesian model class selection was first employed to identify the most plausible class of models for a given set of measurement.

The sequential algorithm (Lam *et al.* 2014) is illustrated here. The evidences for $\boldsymbol{M}_1$ and $\boldsymbol{M}_2$ were calculated using measurement from all four modes (see the "4 modes" part in Table 3) by Eq. (2). The values of the likelihood and Ockham factors (in logarithm) are also presented. The logarithms were used here because the numerical values of the evidence are too large that cause computational problem. Note that the logarithm of likelihood of $\boldsymbol{M}_2$ (1620.71) was much larger than that of likelihood of $\boldsymbol{M}_1$ (-129.97) showing that the model class $\boldsymbol{M}_2$ could fit the measurement better than $\boldsymbol{M}_1$ as expected. The logarithm of Ockham factor of $\boldsymbol{M}_2$ (-27.93) was only a little bit smaller than that of Ockham factor of $\boldsymbol{M}_1$ (-23.18), and the logarithm of overall evidence for $\boldsymbol{M}_2$ (1592.78) was much larger than that of evidence of $\boldsymbol{M}_1$ (-153.15). Therefore, it could be concluded that $\boldsymbol{M}_1$ is not the most plausible model class and the system is damaged. Next, the evidence of $\boldsymbol{M}_3$ was calculated. Since the evidence for $\boldsymbol{M}_3$ was larger than that of $\boldsymbol{M}_2$, the evidence of $\boldsymbol{M}_4$ was needed to be calculated. The logarithm of evidence of $\boldsymbol{M}_4$ (1708.79) was slightly smaller than that of $\boldsymbol{M}_3$ (1714.03). According to the sequential algorithm, the model class $\boldsymbol{M}_3$ was selected as the most plausible model class, and the ballast under the sleeper should be divided into three regions for the purpose of ballast damage detection. This result agreed with the model class employed for generating the measurement.

Next, the Bayesian model updating results using $\boldsymbol{M}_3$ (the most plausible model class) were reported and shown in the "4 modes" part of Table 4. It is clear that the values of $\hat{\theta}_1$, $\hat{\theta}_2$ and $\hat{\theta}_3$ were 0.53, 1.01 and 1.01, respectively, showing that there was a 47% reduction in ballast stiffness in Region 1, while there was no change in ballast stiffness in Regions 2 and 3. The damage detection result can be better interpreted by plotting the ballast stiffness distribution along the target sleeper as shown in Fig. 4. This result matched with the artificial simulated damage in this damaged case. It could be concluded that the proposed ballast damage detection method could successfully identify the ballast damage in damaged case 1 when all four measured modes were included in the analysis. Next, the identified values of other model parameters (also in the "4 modes" part of Table 4) is considered. The identified values for $\hat{\theta}_E$, $\hat{\theta}_L$ and $\hat{\theta}_R$ (i.e., 1.04, 1.59 and 1.56) are almost the same to the values used in simulating the measurement (i.e., 1.04, 1.59 and 1.55). By using the most probable model, the natural frequencies and mode shapes of the rail-sleeper-ballast system in damaged case 1 were calculated and summarized in the "4 modes" part of Table 5 and Fig. 5.

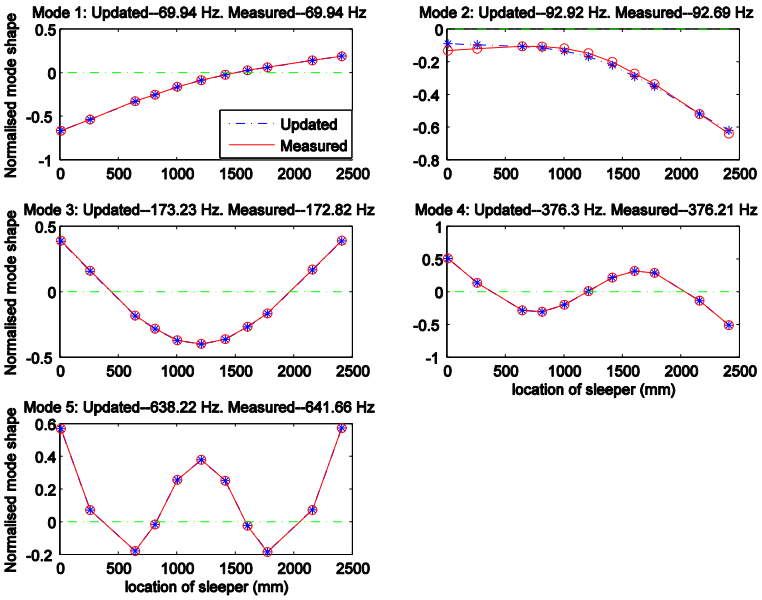

Fig. 5 Matching between measured and model-updated modal parameters using 4 modes

It is clear that the maximum percentage difference between the model-predicted and measured natural frequencies was lower than 0.54%, and the matching between the model-predicted and measured mode shapes was almost perfect. The damage detection results for damaged case 1 using 4 modes with 1% measurement noise are very positive.

Table 3 Evidences of different classes of models in numerical damaged case 1 using different amount of information in model updating

Cases	Class of models	Logarithm of Evidence	Logarithm of Likelihood factor	Logarithm of Ockham factor
4 modes	$\boldsymbol{M}_1$	-153.15	-129.97	-23.18
	$\boldsymbol{M}_2$	1592.78	1620.71	-27.93
	$\boldsymbol{M}_3$	**1714.03**	1746.88	-32.85
	$\boldsymbol{M}_4$	1708.79	1746.22	-37.43
3 modes	$\boldsymbol{M}_1$	1681.88	1702.80	-20.92
	$\boldsymbol{M}_2$	1715.64	1740.80	-25.16
	$\boldsymbol{M}_3$	**1741.58**	1772.93	-31.35
	$\boldsymbol{M}_4$	1736.70	1772.42	-35.72
2 modes	$\boldsymbol{M}_1$	**1749.98**	1771.09	-21.11
	$\boldsymbol{M}_2$	1748.00	1772.85	-24.85
1 mode	$\boldsymbol{M}_1$	**1798.71**	1816.52	-17.81
	$\boldsymbol{M}_2$	1796.75	1816.64	-19.89

Table 4 Optimal parameters in numerical damaged case 1 using different amount of information in model updating

Cases	$\hat{\theta}_1$	$\hat{\theta}_2$	$\hat{\theta}_3$	$\hat{\theta}_E$	$\hat{\theta}_L$	$\hat{\theta}_R$
4 modes ($\boldsymbol{M}_3$)	0.53	1.01	1.01	1.04	1.59	1.56
3 modes ($\boldsymbol{M}_3$)	0.48	1.04	1.02	1.02	1.25	1.64
2 modes ($\boldsymbol{M}_1$)	0.83	---	---	0.72	3.00	0.72
1 mode ($\boldsymbol{M}_1$)	0.55	---	---	0.36	1.18	0.01

Table 5 Measured and model-predicted natural frequencies (Hz) in numerical damaged case 1 using different amount of information in model updating

Cases		Mode 1	Mode 2	Mode 3	Mode 4	Mode 5
4 modes	Updated	69.94	92.92	173.23	376.30	638.22
	Measured	69.94	92.69	172.82	376.21	641.66
	Difference (%)	0.00	-0.25	0.24	-0.02	0.54
3 modes	Updated	69.98	92.73	173.00	373.29	636.58
	Measured	69.94	92.69	172.82	376.21	641.66
	Difference (%)	-0.06	-0.04	-0.10	0.78	0.79
2 modes	Updated	71.15	92.73	153.89	317.44	529.64
	Measured	69.94	92.69	172.82	376.21	641.66
	Difference (%)	-1.73	-0.04	10.95	15.62	17.46
1 mode	Updated	70.03	84.56	119.23	233.07	408.00
	Measured	69.94	92.69	172.82	376.21	641.66
	Difference (%)	-0.13	8.77	31.01	38.05	36.41

3.3 Numerical verification in damaged case 2

Bayesian model class selection by the sequential algorithm was conducted first, and the evidences of different classes of models in damaged case 2 are summarized in Table 6. Model class $\boldsymbol{M}_3$ had the largest evidence among the four model classes, $\boldsymbol{M}_1$, $\boldsymbol{M}_2$, $\boldsymbol{M}_3$ and $\boldsymbol{M}_4$. Therefore, $\boldsymbol{M}_3$ was selected as the most plausible model class in damaged case 2. The updated model parameters are presented in Table 7. The Bayesian model updating results show that the ballast stiffness factor for Regions 1, 2 and 3 are 0.49, 0.50 and 1.00, respectively. Since the simulated damage is 50% reduction in ballast stiffness at Regions 1 and 2, the damage detection result is very positive in damaged case 2 with about 3% error for ballast stiffness at Region 1, and less than 1% error for ballast stiffness at Regions 2 and 3. The Young's modulus and the two additional rail masses were identified with high accuracy. Using the "optimal" model (given in Table 7), the updated

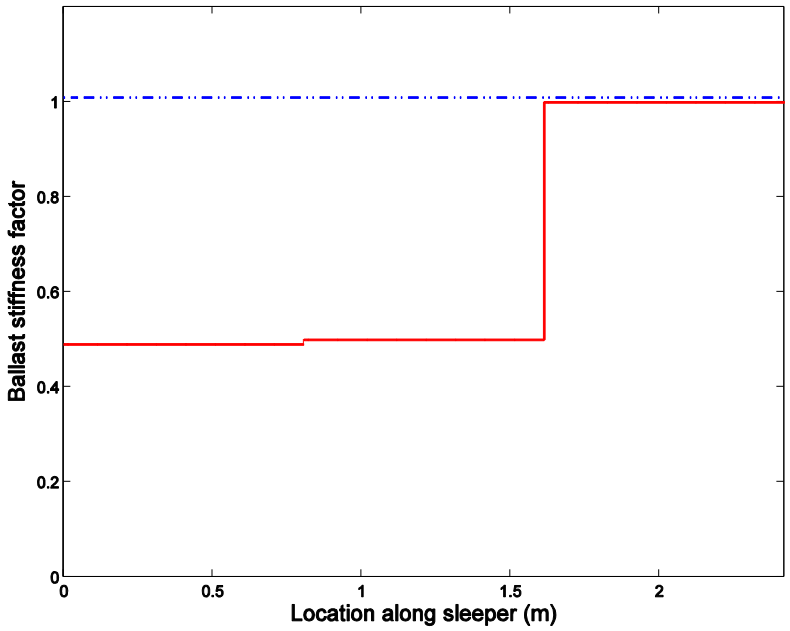

Fig. 6 Damage detection result in Numerical Damaged case 2

modal parameters were calculated. The differences between the measured and model-predicted natural frequencies are shown in Table, where the percentage error was very small in general with the largest error about 2% in mode 1.

The ballast damage detection result is presented by plotting the updated ballast stiffness distribution in Fig. 6. The damage can be easily observed from the figure that the ballast on the left and at the middle of the sleeper with 2/3 the length of the sleeper is damaged, and the percentage reduction in ballast stiffness is almost 50%, which is the same as the simulated damage in damaged case 2 (i.e., 50% reduction at Regions 1 and 2).

3.4 Study the effect of data quantity

The quantity of measured information refers to the number of modes to be considered in the model updating process. Damaged case 1 was employed in this study. The ballast damage detection results for using all four modes were presented in section 3.2. The same ballast damage detection process was repeated using natural frequencies and mode shapes of the first 3, 2 and 1 modes (i.e., less and less measured information). For fair comparisons, the measurement noise level was fixed to 1% in all cases in this study.

Referring to the evidences shown in the "3 modes" part of Table 3, Bayesian model class selection results were similar with that of using the first 4 modes, and the model class $\boldsymbol{M}_3$ was selected as the most plausible model class. The Bayesian model updating results were given in the "3 modes" part of Table 4. Bayesian model updating results showed that the ballast stiffness factor for Region 1 is 0.48, while the factor to the Region 2 is 1.04 and the factor to Region 3 is 1.02. It could be concluded that the proposed ballast damage detection method could detect the ballast damage in damaged case 1 even when only the first 3 modes were included in the analysis. For the optimal values of other model parameters, they were identified with high accuracy except the left rail mass. The percentage error of the left rail mass was 21%. It is not difficult to observe that the accuracy of model updating results in using only 3 modes are not as high as that of model updating results in using 4 modes. For easy comparison, the differences between the measured and model-predicted natural frequencies are shown in the "3 modes" part of Table 5. The largest error in natural frequency was 0.79% in mode 5. It could be concluded that the ballast damage detection results for damaged case 1 using the first 3 modes in the analysis is still very good.

Next only the first 2 modes were considered in the model updating process. The evidences for $\boldsymbol{M}_1$ and $\boldsymbol{M}_2$ were calculated following Eq. (2) and summarized in the "2 modes" part in Table 3. According to the sequential algorithm, the model class $\boldsymbol{M}_1$ was selected as the most plausible model class, and the result indicated that the system was undamaged. It is clear that this model class selection result is wrong when only the first two modes were employed. The Bayesian model updating results using model class $\boldsymbol{M}_1$ were calculated and listed in the "2 modes" part of Table 4. The value of $\hat{\theta}_1$ is 0.83. This result was different from the artificial simulated damage in damaged case 1. The optimal values of other model parameters were identified with relatively low accuracy. The updated Young's modulus was 31% less than the simulated value, the updated left rail mass was 89% higher than the simulated value, and the right rail mass was 54% less than the simulated value. The relatively poor performance when using only the first 2 modes could also be reflected from the differences between the measured and model-predicted natural frequencies as shown in "2 modes" part of Table 5.

Table 6 Evidences of different classes of models in numerical damaged case 2 and experimental case

Cases	Class of models	Logarithm of Evidence	Logarithm of Likelihood factor	Logarithm of Ockham factor
Numerical case 2	$\boldsymbol{M}_1$	-1619.72	-1597.65	-22.07
	$\boldsymbol{M}_2$	1469.62	1496.72	-27.10
	$\boldsymbol{M}_3$	**3043.70**	3075.93	-32.23
	$\boldsymbol{M}_4$	3019.50	3057.22	-37.70
Experimental case	$\boldsymbol{M}_1$	-76.23	-53.94	-22.29
	$\boldsymbol{M}_2$	-73.66	-45.27	-28.39
	$\boldsymbol{M}_3$	**97.22**	124.47	-27.25
	$\boldsymbol{M}_4$	96.73	127.68	-30.95

The differences in natural frequencies in mode 3, 4 and 5 are relatively large and were 11%, 16% and 17%, respectively. The performance of the damage detection method was even worse when only the first mode was considered in the analysis. From the evidences shown in the "1 mode" part of Table 3, it is easy to find that the wrong model class $\boldsymbol{M}_1$ was selected. The Bayesian model updating results were calculated based on $\boldsymbol{M}_1$ and summarized in the "1 mode" part of Table 4. The value of $\hat{\theta}_1$ is 0.55. As expected, the proposed method failed in detecting the ballast damage in damaged case 1 when only the first mode is considered in the analysis. The identification of other model parameters was bad. The updated Young's modulus (0.36) was about 65% less than the simulated value (1.04, refer to Table 1), the updated right rail mass was almost zero while the left rail mass (1.18) is about 26% less than the simulated value (1.59, refer to Table 1). The poor performance could be reflected from the matching among the measured and model-predicted natural frequencies as shown in part 4 "1 mode" of Table 5. It is clear that the errors in all modes except for mode 1, which was the only one included in the model updating, were quite large especially for the modes 3, 4 and 5, where the errors were 31%, 38% and 36%, respectively.

In conclusion, the performance of ballast damage detection is sensitive to the amount of information to be considered in the Bayesian model updating process. According to the results in this numerical case study, at least the first three modes are required for obtaining acceptable damage detection results. This result is in fact reasonable. It is well known that the first two rigid body modes (i.e., modes 1 and 2) are sensitive to the properties of ballast and the two bending modes (i.e., modes 3 and 4) are sensitive to the properties of the sleeper. For the purpose of ballast damage detection, the first two modes are, of course, extremely important. It must be pointed out that the Young's modulus of sleeper and the two rail masses are also considered as uncertain model parameters in the model updating process. Therefore, using only the first two modes is not enough for identifying all uncertain parameters in high accuracy. By including mode 3, which is believed to be sensitive to properties of the sleeper, the model updating result can be improved significantly when compared to that using only the first two modes.

3.5 Study the effect of data quality

This section aims in studying the effects of measurement noise (simulated by introducing a given percentage of root-mean-square white noise to the model-predicted acceleration time-domain responses) in the results of the ballast damage detection. The measurement noise levels of 1%, 5% and 10% were investigated.

Table 7 Optimal parameters in numerical damaged case 2 and experimental case

Cases	$\hat{\theta}_1$	$\hat{\theta}_2$	$\hat{\theta}_3$	$\hat{\theta}_E$	$\hat{\theta}_L$	$\hat{\theta}_R$
Numerical case 2	0.49	0.50	1.00	1.06	1.59	1.56
Experimental case	1.07	0.11	0.99	1.25	0.56	0.01

Table 8 Measured and model-predicted natural frequencies (after model updating) in numerical damaged case 2 and experimental case

Cases	Frequency(Hz)	Mode 1	Mode 2	Mode 3	Mode 4	Mode 5
Numerical case 2	Updated	64.83	87.62	157.06	375.40	639.90
	Measured	63.46	87.61	156.55	374.84	639.04
	Difference (%)	-2.16	-0.01	-0.33	-0.15	-0.13
Experimental case	Updated	60.01	66.90	149.90	407.37	
	Measured	59.84	66.84	153.92	406.09	
	Difference (%)	0.28	0.09	-2.61	0.32	

By following the Bayesian model class selection method, the logarithms of the evidences for different classes of models in damaged case 1 under different noise levels were calculated shown in Table 9 (evidences for 1% noise were extracted from the "4 modes" part of Table 3 for easy comparison). It is clear that the model class $\boldsymbol{M}_3$ was selected in all noise levels. Therefore, the ballast under the sleeper was divided into three regions. By using $\boldsymbol{M}_3$, the Bayesian model updating results for damaged case 1 under different noise levels were calculated and presented in Table 10 (results for 1% noise were extracted from the "4 modes" part of Table 4 for easy comparison). The identified model parameters in all three noise levels were very consistent showing that the effects of measurement noise were not very sensitive to the results of the ballast damage detection.

The differences between the measured and model-predicted natural frequencies under various noise levels were given in Table 11. The differences are very small with values less than 0.5%. Although it was clear that a higher noise level resulted in a relatively lower accuracy in ballast damage detection, the performance of the proposed ballast damage detection method was still very good even under the situation of 10% measurement noise, which indicates that the performance of the proposed ballast damage detection method is not sensitive to the noise level of measurements at the level of 10%.

Table 9 Evidences of different classes of models in numerical damaged case 1 under different noise levels

Noise level	Class of models	Logarithm of Evidence	Logarithm of Likelihood factor	Logarithm of Ockham factor
1%	$\boldsymbol{M}_1$	-153.15	-129.97	-23.18
	$\boldsymbol{M}_2$	1592.78	1620.71	-27.93
	$\boldsymbol{M}_3$	**1714.03**	1746.88	-32.85
	$\boldsymbol{M}_4$	1708.79	1746.22	-37.43
5%	$\boldsymbol{M}_1$	616.11	639.28	-23.17
	$\boldsymbol{M}_2$	1402.20	1430.30	-28.10
	$\boldsymbol{M}_3$	**1452.61**	1486.06	-33.45
	$\boldsymbol{M}_4$	1446.29	1484.47	-38.18
10%	$\boldsymbol{M}_1$	1061.12	1082.80	-21.68
	$\boldsymbol{M}_2$	1290.77	1317.41	-26.64
	$\boldsymbol{M}_3$	**1343.66**	1375.58	-31.92
	$\boldsymbol{M}_4$	1340.97	1377.31	-36.34

Table 10 Optimal parameters in numerical damaged case 1 under different noise levels

Noise level	$\hat{\theta}_1$	$\hat{\theta}_2$	$\hat{\theta}_3$	$\hat{\theta}_E$	$\hat{\theta}_L$	$\hat{\theta}_R$
1%	0.53	1.01	1.01	1.04	1.59	1.56
5%	0.56	0.96	1.02	1.04	1.58	1.58
10%	0.57	1.00	1.01	1.03	1.51	1.58

Table 11Measured and model-predicted natural frequencies in numerical damaged case 1 under different noise levels

Noise level	Frequency(Hz)	Mode 1	Mode 2	Mode 3	Mode 4	Mode 5
1%	Updated	69.94	92.92	173.23	376.30	638.22
	Measured	69.94	92.69	172.82	376.21	641.66
	Difference (%)	0.00	-0.25	0.24	-0.02	0.54
5%	Updated	71.20	92.68	171.93	376.30	638.04
	Measured	71.26	92.64	171.99	375.99	643.62
	Difference (%)	0.08	-0.04	0.03	-0.08	0.87
10%	Updated	72.34	92.69	172.97	375.11	636.51
	Measured	72.30	92.65	172.35	375.44	644.18
	Difference (%)	-0.06	-0.04	-0.36	0.09	1.19

4. Experimental verification

In this section, the proposed ballast damage detection methodology was verified through experimental measured data from the indoor test panel as shown in references (Lam *et al*. 2012, 2014). Ballast damage was simulated under the middle of the sleeper by replacing normal size ballast (~50 mm) by small size ballast (~15 mm). Natural frequencies and mode shapes of the first four modes were identified (using MODE-ID) from the measured responses in the roving hammer test.

Bayesian model class selection and model updating were conducted using the identified modal parameters. The Bayesian model class selection results were summarized in Table 6. The model class $\boldsymbol{M}_3$ is selected as the most probable model because it has the largest logarithm of evidence (97.22) among all the considered model classes. The model updating results are summarized in Table 7. The ballast under the sleeper was divided into three regions with the corresponding ballast stiffness values θ_1, θ_2 and θ_3. The identified ballast stiffness factors for the left, middle and right regions are 1.07, 0.11 and 0.99, respectively. As the ballast stiffness at the middle region dropped significantly, the proposed method detected the ballast damage under the middle of the sleeper. The ballast damage detection result can be better presented by plotting the updated ballast stiffness distribution in Fig. 7. The damage can be easily found and it was located at the middle part of the sleeper, the percentage reduction in ballast stiffness was about 86%. The differences between the measured and updated natural frequencies are given in Table 8. the largest error is 2.61% in mode 3 and the matching is good. Therefore, the proposed ballast damage detection methodology successfully detected the damage in the experimental case.

5. Conclusions

This paper reports the development of a railway ballast damage detection method utilizing roving hammer test data following the Bayesian model class selection and model updating method. To handle the problem of local optima in model updating, the two-stage hybrid optimization method was developed with the modified evolutionary algorithm.

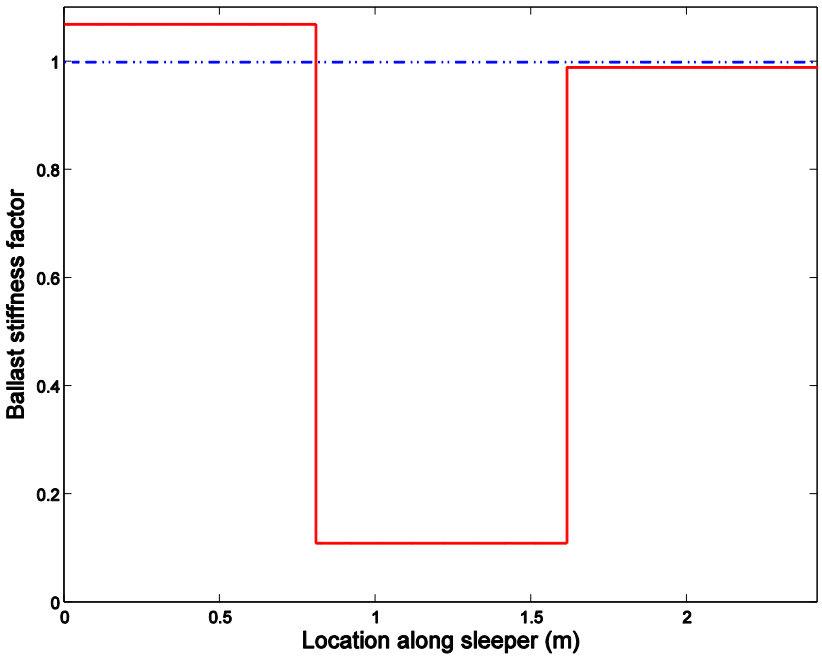

Fig. 7 Damage detection result in experimental case

The proposed ballast damage detection method successfully identified the simulated ballast damage in both numerical and experimental cases. Based on a comprehensive numerical case studies, the effects of the quantity and quality of measurement on the results of ballast damage detection were studied. The results show that the amount of information (data quantity) to be considered in the model updating process plays an important role in ballast damage detection. At least the first three modes are required to obtain acceptable damage detection results. Furthermore, the performance of the proposed ballast damage detection method was not sensitive to the level of measurement noise (data quality). As shown in the study, the ballast damage detection results are very good even with 10% measurement noise.

The proposed methodology requires only 1 accelerometer and 1 impact hammer with load cell for collecting vibration data. Therefore, it is believed that the method is suitable for permanent way engineers or inspectors to get additional information about ballast situations under concrete sleepers during visual inspection.

The next step of this research is to extend the proposed ballast damage detection method using train-induced vibration in-situ sleeper. This is one important step in the development of a smart system for long-term monitoring of railway ballast of a track by installing accelerometers on a number of selected sleepers. Several difficulties must be overcome before this extension can be implemented. The main difficulty is that the stress-strain behavior of ballast may become nonlinear under the action of train load (large amplitude vibration). This difficulty can be addressed by modifying the methodology from using modal-domain to time-domain data, and develop a nonlinear model to capture the dynamic behavior of railway ballast. Furthermore, an optimal sensor configuration method needs to be developed for selecting a set of appropriate sleepers for installing sensors in order to maximize the amount of information that can be extracted for the purpose of ballast damage detection.

From the literature (e.g., Xia *et al.* 2006, 2012), it is believed that an increase in temperature in general will reduce the natural frequencies of a reinforced concrete structure. Therefore, it is believed that the modal parameters of the in-situ sleeper may be changed due to temperature changes. Before the proposed method can be put into real application, the effects of temperature on the performance of the proposed method must be studied. This can be done through comprehensive experimental case studies in the indoor test panel under various temperatures through the air-conditioning system.

Acknowledgements

The work described in this paper was fully support ed by the grant from the Research Grants Council of t he Hong Kong Special Administrative Region, China [Project No. CityU 115413 (9041889)], Basic Research Program of China (Project No. 2016YFC0802002), Nati onal Nature Science Foundation of China (NSFC, Proje ct No. 51629801) and from the Fundamental Research Funds for the Central Universities (HUST: 2017KFYXJ J137). The authors would also like to thank the anonymous reviewers for their constructive comments and suggestions.

References

An, D., Choi, J.H. and Kim, N.H. (2011), "Identification of correlated damage parameters under noise and bias using Bayesian inference", *Struct. Health Monit.*, **11**(3), 293-303.

Au, S.K. (2011), "Fast Bayesian FFT method for ambient modal identification with separated modes", *J. Eng. Mech*., **137**(3), 214-226.

Back, T. (1996), *Evolutionary Algorithms in Theory and Practice: Evolution Strategies, Evolutionary Programming, Genetic Algorithms*, Oxford university press, 1st Ed., New York, USA.

Beck, J.L. (1978), "Determining models of structures from earthquake records", Ph.D. Dissertation, California Institution of Technology, USA.

Beck, J.L. and Katafygiotis, L.S. (1998), "Updating models and their uncertainties I: Bayesian statistical framework", *J. Eng. Mech. - ASCE*, **124**(4), 455-461.

Beck, J.L. and Yuen, K.V. (2004), "Model selection using response measurement: Bayesian probabilistic approach", *J. Eng. Mech. - ASCE*, **130**(2), 192-203.

Berggren, E. (2009), "Railway track stiffness-dynamic measurements and evaluation for efficient maintenance", Ph.D. Dissertation, Royal Institute of Technology (KTH), Sweden.

Box, G.E.P. and Tiao, G.C. (1973), *Bayesian inference in statistical analysis*, Addision-Wesley, Reading, Mass.

Cao, Z.J. and Wang, Y. (2014), "Bayesian model comparison and selection of spatial correlation functions for soil parameters", *Struct. Saf.*, **49**, 10-17.

Fujino, Y., Siringoringo, D.M. and Abe, M. (2009), "The needs for advanced sensor technologies in risk assessment of civil infrastructures", *Smart Struct. Syst.*, **5**(5), 173-191.

Fan, W. and Qiao, P.Z. (2011), "Vibration-based damage identification methods: a review and comparative study", *Struct. Health Monit.*, **10**(1), 83-111.

Hu, Q. (2015), "Bayesian ballast damage detection in consideration of uncertainties from measurement noise and modelling error", Ph.D. Dissertation, City University of Hong Kong, Hong Kong.

Hu, Q. and Lam, H.F. (2012), "Model updating of the rail-sleeper-ballast system and its application in ballast damage detection". Proceedings of the *7th Australasian Congress on Applied Mechanics (ACAM 7)*, Adelaide, Australia, 9-12 December.

Hu, Q., Lam, H.F. and Alabi, S.A. (2015), "Use of measured vibration of in-situ sleeper for detecting underlying railway ballast damage", *Int. J. Struct. Stab. Dynam.*, **15**(8), 1540026(1-14).

Jeffreys, H. (1961), *Theory of probability*. 3rd ed. Clarendon, Oxford, U.K..

Jo, H.K., Park, J.W., Spencer, B.F. and Jung, H.J. (2013), "Development of high-sensitivity wireless strain sensor for structural health monitoring", *Smart Struct. Syst.*, **11**(5), 477-496.

Kaewunruen, S. and Remennikov, A.M. (2009), "Application of vibration measurements and finite element model updating for structural health monitoring of ballasted railtrack sleepers with voids and pockets", *Faculty of Engineering-Papers.*

Krenk, S. (2001), *Mechanics and Analysis of Beams, Columns and Cables: a Modern Introduction to the Classic Theories*. Springer Science & Business Media.

Kuok, S.C. and Yuen, K.V. (2012), "Structural health monitoring of Canton Tower using Bayesian framework", *Smart Struct. Syst.*, **10**(4-5), 375-391.

Lam, H.F., Hu, Q. and Wong, M.T. (2014), "The Bayesian methodology for the detection of railway ballast damage under a concrete sleeper", *Eng. Struct.*, **81**, 289-301.

Lam, H.F., Ng, C.T. and Leung, A.Y.T. (2008), "Multicrack detection on semirigidly connected beams utilizing dynamic data", *J. Eng. Mech.*, **134**(1), 90-99.

Lam, H.F., Ng, C.T. and Veidt, M. (2007), "Experimental characterization of multiple cracks in a cantilever beam utilizing transient vibration data following a probabilistic approach", *J. Sound Vib.*, **305**(1-2), 34-49.

Lam, H.F., Wong, M.T. and Keefe, R.M. (2010), "Detection of ballast damage by in-situ vibration measurement of sleepers", *Proceedings of the 2nd International Symposium on Computational Mechanics and 12th International Conference on Enhancement and Promotion of Computational methods in Engineering and Science*, **1233**(1), 1648-1653. AIP Publishing.

Lam, H.F., Wong, M.T. and Yang, Y.B. (2012), "A feasibility study on railway ballast damage detection utilizing measured vibration of in situ concrete sleeper", *Eng. Struct.*, **45**, 284-298.

Lam, H.F. and Yin, T. (2010), "Statistical detection of multiple cracks on thin plates utilizing dynamic response", *Eng. Struct.*, **32**(10), 3145-3152.

Muto, M. and Beck, J.L. (2008), "Bayesian updating and model class selection for hysteretic structural models using stochastic simulation", *J. Vib. Control*, **14**(1-2), 7-34.

Meyer, J., Bischoff, R., Feltrin, G. and Motavalli, M. (2010), "Wireless sensor networks for long-term structural health monitoring", *Smart Struct. Syst.*, **6**(3), 263-275.

Ni, Y.C., Zhang, F.L., Lam, H.F. and Au, S.K. (2015), "Fast Bayesian approach for modal identification using free vibration data, Pat II-Posterior uncertainty and application", *Mech. Syst. Signal. Pr.*, **70-71**, 221-244.

Ni, Y.Q., Li, B., Lam, K.H., Zhu, D.P., Wang, Y., Lynch, J.P. and Law, K.H. (2011), "In-construction vibration monitoring of a super-tall structure using a long-range wireless sensing system", *Smart Struct. Syst.*, **7**(2), 83-102.

Ni, Y.Q., Xia, Y., Lin, W., Chen, W.H. and Ko, J.M. (2012), "SHM benchmark for high-rise structures: a reduced-order finite element model and field measurement data", *Smart Struct. Syst.*, **10** (4-5), 411-426.

Nagayama, T., Sim, S.H., Miyamori, Y. and Spencer, B.F. (2007), "Issues in structural health monitoring employing smart sensors", *Smart Struct. Syst.*, **3**(3), 299-320.

Papadimitriou, C., Beck, J.L. and Katafygiotis, L.S. (1997), "Asymptotic expansions for reliability and moments of uncertain systems", *J. Eng. Mech.*, **123**(12), 1219-1229.

Przemieniecki, J.S. (1985), *Theory of Matrix Structural Analysis*. Courier Corporation.

Selig, E.T. and Waters, J.M. (1994), *Track Geotechnology and Substructure Management*. Thomas Telford.

Salawu, O.S. (1997), "Detection of structural damage through changes in frequency: a review", *Eng. Struct.*, **19**(9), 718-723.

Vanik, M.W., Beck, J.L. and Au, S.K. (2000), "Bayesian probabilistic approach to structural health monitoring", *J. Eng. Mech.*, **126**(7), 738-745.

Worden, K. and Hensman, J.J. (2012), "Parameter estimation and model selection for a class of hysteretic systems using Bayesian inference", *Mech. Syst. Signal. Pr.*, **32**, 153-169.

Xia, Y., Chen, B. and Weng, S., Ni, Y.Q. and Xu, Y.L. (2012), "Temperature effect on vibration properties of civil structures: a literature review and case studies", *Civ. Struct. Health Monit.*, **2**(1), 29-46.

Xia, Y., Hao, H., Zanardo, G. and Deeks, A. (2006), "Long term vibration monitoring of an RC slab: temperature and humidity effect", *Eng. Struct.*, **28**(3), 441-452.

Yuen, K.V. and Lam, H.F. (2006), "On the complexity of artificial neural networks for smart structures monitoring", *Eng. Struct.*, **28**(7), 977-984.

Yuen, K.V. (2010), *Bayesian methods for structural dynamics and civil engineering*. John Wiley& Sons, New York.

Zhang, F.L., Ni, Y.C. and Au, S.K. and Lam, H.F.(2015), "Fast Bayesian approach for modal identification using free vibration data, Part I – Most probable value", *Mech. Syst. Signal. Pr*., **70-71**, 209-220.

FC